A SIMULATION ENVIRONMENT FOR THE EVALUATION OF AIRBORNE BISTATIC RADAR CONCEPTS FOR EXTERNAL HAZARD DETECTION

Roland W. Lawrence, Old Dominion University

Abstract

A simulation tool to aid in evaluating bistatic or passive radar concepts was developed in this study. The modular simulation environment was based on existing Electromagnetic (EM) models and provides an estimate of the atmospheric propagation and surface scattering for frequencies from 1 to 40GHz. A key attribute of this simulation environment was its flexibility and expandability. The approach was to develop modules that could be integrated into existing modeling environments such as MATLAB or OCTAVE to model EM propagation, emissions and scattering, as well as the operation of microwave instruments and data-processing concepts. The overall simulation capability can be modified by researchers and expanded for specific applications. This study focused on the development of a flexible framework and a set of EM modules that ccould be used to demonstrate the capability.

The objective of this study was to develop a tool with broad capability to enable the assessment of varied sensor technologies for detection of aircraft hazards. However, to demonstrate the capability of the simulation environment, an airborne bistatic radar concept using Direct Broadcast Satellite (DBS) as the illuminator was modeled and is presented in this paper. The paper will also provide an overview of the simulation environment and a description of the atmospheric loss model, surface-scattering model, and rain-scattering model used to demonstrate the capability and the results of the DBS bistatic simulation.

Background

The use of bistatic, or passive, radar concepts that utilize existing transmitters or emitters-of-opportunity have seen interest recently in a wide range of applications. The use of reflected signals from Global Positioning System (GPS) satellites to measure wind speed over water and soil moisture have been studied, and techniques to utilize bistatic radar to detect and track aircraft have also been developed [1-4]. Research is also underway to infer local wind fields from ground-based bistatic radar measurements utilizing dedicated radar transmitters [5]. It may be possible to extend this earlier work to develop an airborne bistatic radar concept utilizing emitters-of-opportunity with varied frequencies and polarizations to augment existing aircraft weather radars in the detection of severe weather hazards. These measurements could be used to augment existing aircraft radars for the detection of convective storm processes and wind-field structures and may be suitable for the detection of hazards such as gust fronts, cross winds, and other potentially dangerous artifacts of the wind field. Bistatic radar measurements may also be used for the detection of other aircraft or runway incursion. The advantages and limitations of such bistatic concepts are not well understood, and a simulation environment is needed to investigate the potential utility of such a sensor concept.

Several researchers have developed EM propagation and scattering models in support of the evaluation of bistatic radars [4]. The EM propagation and scattering models are typically focused on the specific-instrument concept. For example, a high-fidelity scattering model may be developed that has application only over a narrow range of frequencies. The effort discussed here is focused on developing a model with very broad applicability, albeit with lower fidelity, to enable the rapid assessment of new microwave sensor concepts and technologies. A model with this broad capability may enable the relative performance of two sensor concepts to be estimated and needed technologies to be identified. In addition, such a capability would allow the fusion of data from multiple sensors to be more easily studied. The long-term goal of this research project is to develop a flexible EM-simulation environment that can be easily modified and extended as needed to enhance the study of new microwave-sensor concepts and technologies.

Approach

The simulation environment was formed using modules based on MATLAB/OCTAVE modeling software. The modules were developed using existing EM-propagation, surface-scattering, and precipitation-scattering models. These were necessary in order to develop a useful simulation environment for frequencies from 1 to 40GHz. In addition, a data structure was developed to provide a uniform data interface between the modules. The developed data structures allow for easy upgrade of individual models and provide management of the bistatic scattering geometry with minimum impact on the overall simulation. A simplified block diagram of the simulation environment is shown in Figure 1.

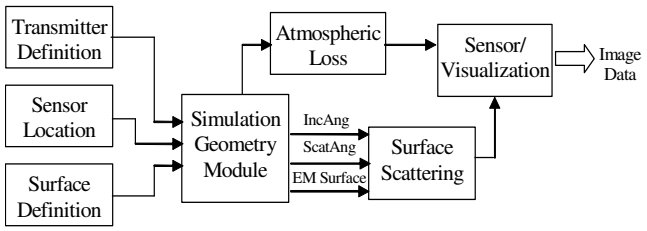

Figure 1. Simulation environment simplified Block diagram

The transmitter, sensor, and scene information were used to determine the angle of incidence of the transmitted signal and the scattered angle toward the sensor for each surface pixel. This data, along with the EM characteristics of the surface for each pixel, were formed into matrices of data structures that could then be passed as inputs to the EM and visualization modules. The rows and columns of these matrices correspond to the surface pixels, and the corresponding data structure provides the information required by the scattering model to calculate the signal from the illuminating transmitter scattered toward the receiver by that surface pixel.

The simulation environment shown in Figure 1 can serve as a framework for advanced aircraft-sensor research. The Simulation Geometry Module essentially provides the coordinate system of the environment and allows the EM characteristics of the surface or simulated atmosphere to be specified. This is the core of the EM simulation environment. A Transmitter Definition Module specifies the location, polarization, frequency, etc. of the transmitter of interest. The Atmospheric Propagation Module and scattering modules for the surface and hydrometeors then form a working end-to-end simulation. Finally, an aircraft, or sensor, is then positioned in the scene and a sensor can "observe" the reflected signal from any point in the scene. A major advantage of this modular approach is that simple models can be quickly developed to demonstrate their capability and the modules can be later modified to extend their applicability or improve their fidelity as required.

While clearly the goal is for researchers to expand the simulation tool and apply it to a variety of sensor concepts, the simulation of the bistatic scattering of the Direct Broadcast Satellite (DBS) TV signal from the area around an airport will be used in this paper to demonstrate the initial microwave simulation tool. A brief description of the simulation environment is provided in the next section. In some cases, the EM model or Module may have capability that was not required or used in the test case of this study.

Simulation Environment Description

The Simulation Geometry Module defines the coordinate system and the EM characteristics of all regions within the simulation space. In addition, the location of the transmitter and the aircraft, as well as the scan and elevation angle of the sensor antenna, were maintained in this module. The geometry of the simulation is illustrated in Figure 2. The surface of the Earth is assumed to be in the xy plane and the altitude of an aircraft in measured along the z-axis. The location of the aircraft, terrestrial transmitters, and objects in the simulation are specified by their (x y z) coordinates. Azimuth directions such as the aircraft flight direction are specified as a compass bearing, where North is defined as the +y-axis. Various utility functions are available to find distances and bearings between points and a simple "surface editor" allows the user to specify the EM characteristics of different regions of the surface.

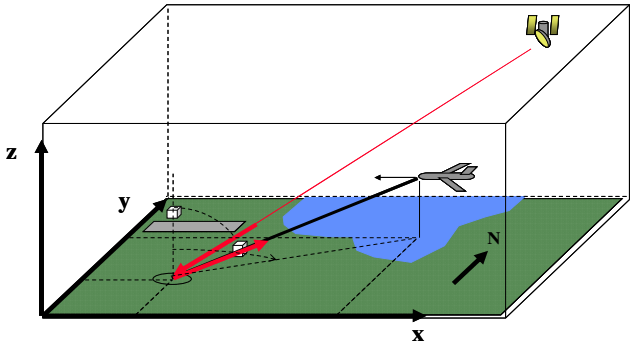

Figure 2. The geometry of the EM Hazard simulation is maintained by the Simulation Geometry Module

Based on the location of the transmitter, aircraft, and the scan angle of the sensor, the incidence angle of the illumination and the scattering angle to the aircraft were calculated. The appropriate bistatic scattering model was then selected for the imaged surface cell (or pixel). The Simulation Geometry Model then calls the Atmospheric Model to determine the losses due to water vapor and oxygen for the propagation paths. The microwave image of a scene illuminated by a signal of opportunity and observed from an aircraft can then be approximated.

The atmospheric model developed in this study provided the propagation and atmospheric losses for frequencies from 1 to 40GHz. For this frequency range, only absorption due to water vapor and oxygen molecules were significant. The attenuation will change significantly over this range (near 22GHz). More importantly, absorption of EM energy by molecules of water vapor and oxygen in the atmosphere due

to the coupling of rotation modes may be important for some microwave measurement approaches in this frequency range. Thus, this phenomenon was explicitly included in the model. Although the atmospheric loss was not of interest for the initial DBS simulation, the module will clearly be important for future investigations and is discussed below.

While the absorption due to individual molecules can be calculated, the situation in the atmosphere includes many molecules and the interaction and collisions between these gas molecules results in a modification of the absorption, essentially broadening the absorption line. This substantially complicates the absorption calculation. The approach that has been successfully applied in atmospheric remote sensing at microwave frequencies is to develop a line-shape function to capture this broadening of the absorption line. These functions are typically a function of temperature and pressure and model the effect of pressure broadening of the line [6], [7]. By combining the attenuation for absorption lines in the frequency range of interest for water vapor and oxygen, the atmospheric absorption coefficient can be approximated.

The coefficients in the above models are typically empirically adjusted to fit experimental data. The approach used here to model the water vapor (WV) and oxygen (O_2) absorption was developed by Liebe & Dillon [7]. The absorption coefficient for WV can be written [6]

$$\kappa_{H_2O}(f) = 2f^2\rho_v\left(\frac{300}{T}\right)^{1.5}\gamma_l \times\left[\left(\frac{300}{T}\right)e^{-644/T}\left(\left(494.4-f^2\right)^2+4f^2\gamma_l^2\right)^{-1}+1.2\times10^{6}\right] \text{ dB/km} \quad (1)$$

where the line width parameter was found to be

$$\gamma_l = 2.85\left(\frac{P}{1013}\right)\left(\frac{300}{T}\right)^{0.626}\times\left[1+0.18\left(\frac{\rho_v T}{P}\right)\right] \text{ GHz} \quad (2)$$

and where f is the frequency in GHz, T is the temperature in Kelvin, P is pressure in mbar, and ρ_v is the water vapor in gr/m^3.

A similar approach was used to characterize the absorption due to O_2. For frequencies below 40GHz, the effect of the oxygen absorption complex at 60GHz can be approximated by a residual term as for the 183GHz water-vapor line in the development of equation (1). Thus, if O_2 absorption is ignored by lines above 60GHz and the absorption is approximated as a single line at 60GHz, the O_2 absorption can be written [6] as

$$\kappa_{O_2}(f) = 0.011f^2\left(\frac{P}{1013}\right)\left(\frac{300}{T}\right)^2\times\gamma\left[\left((f-60)^2+\gamma^2\right)^{-1}+\left(f^2+\gamma^2\right)^{-1}\right] \text{ dB/km} \quad (3)$$

where the line width parameter was determined [8] to be

$$\gamma = \left(\frac{P}{1013}\right)\left(\frac{300}{T}\right)^{0.85}\times\begin{cases}0.59 & P\geq 333 \text{ mbar}\\ 0.59\left[1+0.0031(333-P)\right], & 25\leq P\leq 333 \text{ mbar}\\ 1.18 & P\leq 25 \text{ mbar}\end{cases} \text{ dB/km} \quad (4)$$

Combining equations (1) and (3), the total atmospheric absorption for frequencies between 1 and 40GHz could be found. The modeled propagation loss due to WV and O_2 is shown in Figure 3.

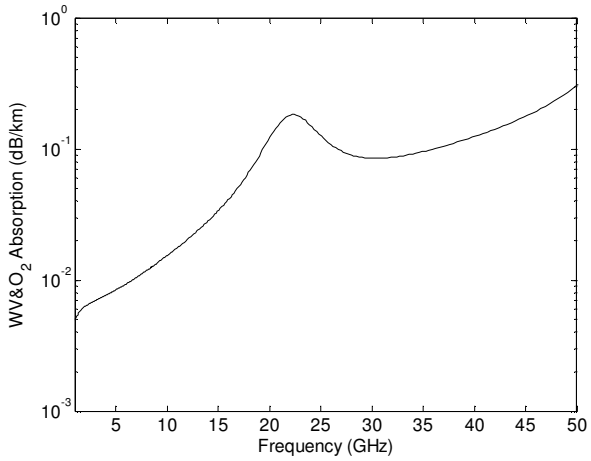

Figure 3. Atmospheric absorption due to WV and O_2

Next, the bistatic scattering coefficient at the surface must be calculated to find the power scattered in the direction of the aircraft. Scattering from terrain is a rather complex phenomenon and may include volume scattering from vegetation or surface scattering, where the scattering occurs only from the surface of a rough plane. As the complexity of the terrain-scattering model is increased to accommodate a more general scene, it will quickly reach a point where the model becomes cumbersome and may exceed the capability of an average desktop computer. The approach used here was to develop a suite of surface-scattering models for classes of terrain that are sufficient to develop a representative microwave scene but are computationally efficient. The modules can be modified or augmented as future needs dictate. Eventually a library of terrains will be available and the user can assign various surfaces, such as concrete, grass, forest, or water, to locations on the surface using the "surface editor".

The Kirchhoff approximation has been widely used to describe the scattering from surfaces where horizontal variations occur slowly compared to the wavelength [9]. That is, the surface can be viewed as being formed from tilted facets and the total field at a point can be calculated as if the surface were an infinite plane tangent to the surface at that point. If, in addition, a Gaussian surface height with a large standard deviation relative to the wavelength is assumed,

then the stationary phase approximation can be used and an analytic approximation for the scattering can be obtained [10].

Using this approach, a MATLAB/OCTAVE function was developed to calculate a bistatic scattering coefficient as a function of rms slope of the surface and dielectric constant of the surface for each surface pixel. In this function, the elevation incidence angle, θ, was measured from zenith (normal to the xy plane) or measured in the plane of incidence, and the incidence azimuth angle, ϕ, from the y-axis (or North in the simulation). The elevation scattered angle, θ_s, was measured from the z-axis and in the plane including the scattering point, P, and the receiver. The scattered azimuth angle was measured from the y-axis.

Setting $\phi = \phi_s$, the backscatter can be calculated and compared to other models. The model was used to approximate the backscattering coefficient for a surface with a dielectric constant of 1.6 for rms surface slopes ranging from 0.1 to 0.4. The results are shown as a function of angle of incidence in Figure 4. The backscatter decreases with increasing incidence angle and decreases more slowly as the surface becomes more rough, as expected. The results in Figure 4 agree well with similar models [6].

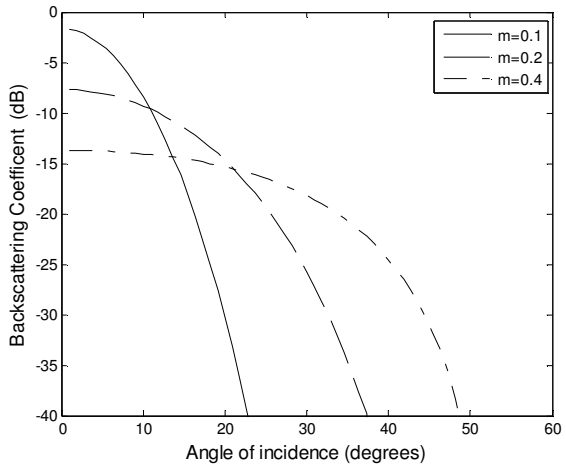

Figure 4. Backscatter Coefficient

The model can also be used to approximate the bistatic scattering from a rough soil for the DBS signal at 12GHz. The dielectric constant for soil at 12GHz varies between approximately 2.0, for very dry soil, and 12 for very wet soil. These values also are a function of soil type but this range was suitable for our demonstration. The bistatic scattering coefficient was calculated for these surfaces assuming illumination from the DBS satellite, $\theta = 50°$, and for observing aircraft on a 3° glide slope, $\theta s = 87°$. Further, the scattering was calculated for surfaces with three different rms surface slopes to simulate portions of the scene with varying roughness. The simulated bistatic scattering coefficient as a function of scattering azimuth angle, ϕ_s is shown in Figure 5. The incidence azimuth angle, ϕ, was set to zero in the

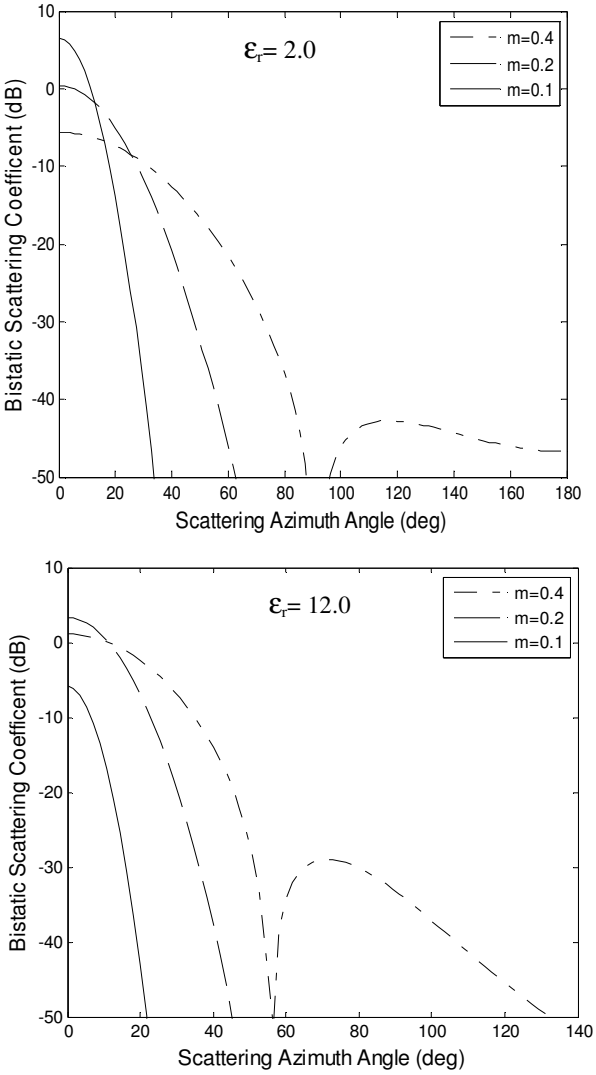

Figure 5. Bistatic scattering coefficient

calculation. Therefore, $\phi_s = 0$ corresponds to forward scattering and $\phi_s = 180$ to back scattering.

A few comments regarding Figure 5 may be helpful. The bistatic scattering coefficient illustrated in the Figure 5 describes the DBS signal that is scattered toward an elevation angle of $\theta_s = 87°$. Since ϕ has been set to zero, the azimuth scattering angle can be interpreted as the azimuth angle from the plane of incidence to the scattered azimuth direction (3° above the horizon, in the direction of an aircraft on a 3° glide

slope). As can be seen in Figure 5, most of the DBS signal is forward-scattered and the less rough the surface the more the power is forward-scattered. Figure 5 also illustrates the dependence of the scattering coefficient on the surface dielectric constant. The variation in the scene may be quite large due to variation in the soil type, soil moisture, and roughness (note vegetation was not considered). It also appears from Figure 5 that once the scattering azimuth angle is more than about 20° from the plane of incidence (forward scattering) the surface roughness appears to be the dominate factor in the scattering coefficient.

The surface-scattering model, atmospheric propagation model, and the simulation geometry module can then be combined to estimate the DBS signal scattered toward an aircraft on final approach. A terminal area scene can be built from a matrix of cells, each with surface dielectric constant and roughness parameters defined by the user. This approach can be used to provide the surface-clutter environment for the investigation of the performance of a bistatic rain model to detect weather hazards or, with some improvements, surface scattering may directly provide other useful hazard information.

To enable the simulation of hazardous weather in the terminal area, an approximation for EM scattering from areas of rain is needed. The scattering from precipitation will be a function of the drop-size distribution and the frequency of the incidence signal. Rayleigh scattering is usually assumed for drop sizes less than approximately a tenth of a wavelength. Drop sizes in heavy rain rate may exceed 2.0mm [11]. Thus, for larger rain rates, the Rayliegh approximation may not be appropriate for frequencies above about 15GHz. The calculation to apply Mie scattering theory can be numerically intensive so an approximation was adapted from an alternate approach [12] and developed for this simulation.

The general approach used here was to modify the reflectivity factor, Z, used in the Rayliegh formulation for the radar cross section in equation 5

$$\sigma_{rain} = 10^{-10}\left(\frac{\pi^5}{\lambda^4}\right)K_w{}^2 Z \tag{5}$$

where λ is the wavelength in cm, K_w is the dielectric constant for water (approximately 0.9 for $0<T<18^0$C), and Z is the reflectivity factor modified to include Mie scattering. Wexler and Atlas [12] used results of a more complex scattering model including both Rayliegh and Mie scattering over several frequency ranges along with an assumed drop-size distribution (Marshall-Palmer) to form an effective reflectivity factor including the effects of Mie scattering. The relationship between this effective reflectivity factor and rain rate, as shown in Table 1, was adapted from work done by Wexler & Atlas [12]. These relationships agree well with the Rayliegh approximation for wavelengths 3.2 to 10cm. For wavelengths less than 1.24cm, the effect of Mie scattering can be seen in the effective reflectivity especially for larger rain rates. A "look up" table with interpolation between wavelengths was included in the simulation to approximate the scattering from severe weather in the terminal area.

Table 1. Mie corrected reflectivity factor $Z=\eta R^{\zeta}$

Wavelength (cm)	Range of R (mm/hr)	η	ζ
0.62	0-5	240	1.1
	2-20	345	0.9
	20-100	540	0.75
0.86	0-5	350	1.32
	5-20	450	1.15
	20-100	780	0.95
1.24	0-5	356	1.5
	5-20	460	1.35
	20-100	820	1.15
1.87	0-20	330	1.54
	20-50	500	1.4
	50-100	750	1.3
3.21	0-100	275	1.55
4.67	0-100	280	1.45
5.5	0-100	280	1.45
10	0-100	295	1.45

Results

A simulation of the observed bistatic scene illuminated by a Direct Broadcast Satellite (DBS) and observed from an aircraft on final approach was used to demonstrate the capability of the modeling environment. The scene was created using several of the modules discussed above. The demonstration scene included a concrete runway surrounded by moderately rough terrain. In addition, two bodies of water with surface roughnesses associated with lakes and an area of rough terrain were included to demonstrate the utility of the model. Rain cells were later added to explore the ability of simulating severe weather in the terminal area. The simulations shown here are for a scene illuminated by a Direct Broadcast Satellite, where the frequency was 12GHz and the incidence angle was 40^0. The azimuth angle to the illuminating satellite varied in the simulation to assess the impact of changes in the orientation of the aircraft and runway. The EM properties of the surface, dielectric constant and normalized rms slope of the surface were entered for the surface-scattering model. The illumination and observation positions, and aircraft location, were then used to find the DBS signal scattered in the direction of the aircraft (or receiver). A description of these surface regions and the EM properties used in the demonstration are shown in Figure 6. The aircraft, located in the center of the scene on approach to the runway (~3^0 glide slope), is shown in the image. The incidence angle of the illumination was 40^0 and the azimuth

angle of the illuminating satellite was varied in the simulations.

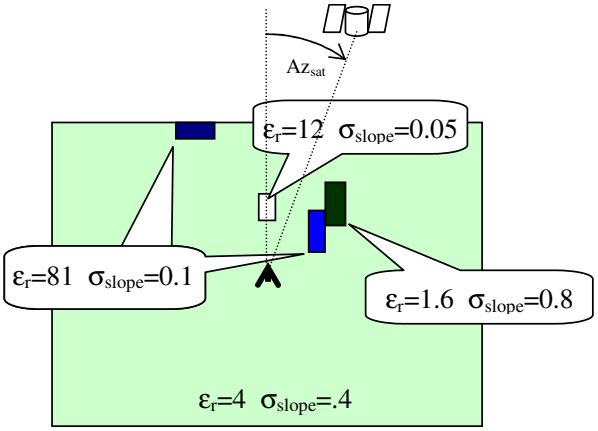

Figure 6. Surface regions uses in demonstration

The simulated bistatic scattering from the satellite to the aircraft location is shown in Figure 7 for several illumination angles. Az = 0^0 illustrates the forward scattering case. In this image, the less rough regions in front of the aircraft (concrete runway and lakes) reflect less signal toward the aircraft (appearing "cooler in image"). This was to be expected since smoother surfaces reflect more energy in the specular direction. The forward-scattering case appears to provide less contrast for the rough terrain located just to the right of the runway. The scattering geometry of the Az_{sat} = 90^0 image has the surface illuminated 90^0 from the aircraft course. In this image, the aircraft is even further from the specular direction and the smooth runway and lakes scatter even less power toward the aircraft. The Az_{sat}=135^0 image suggests improved contrast for the rough-terrain region to the right of the runway. This is due to a reduction in the scattered signal from the smoother surrounding areas when the illumination is behind the observer. In addition, the contrast between the surrounding areas and the smoother runway and lake regions also improves when the illumination is behind the observer since these more specular surfaces provide even less backscatter towards the aircraft.

A coordinate transformation is available to produce a sensor/aircraft view of the simulated scene. A rain event was added to the scene with a rain rate ranging from 30 to 10mm/hr. The results are shown in the sensor/aircraft view in Figure 8. The illumination azimuth is 180^0 (directly behind the scene). As expected with the illumination behind the sensor, the smooth surfaces and the rough region to the right of the runway are clearly visible in the image. The rain cells can also be identified in the image. Substantial contrast exists between the smooth runway and the scattering from the rain. However, it appears that for moderate surface roughness, the scattered DBS signal from the rain and the surface may be very similar.

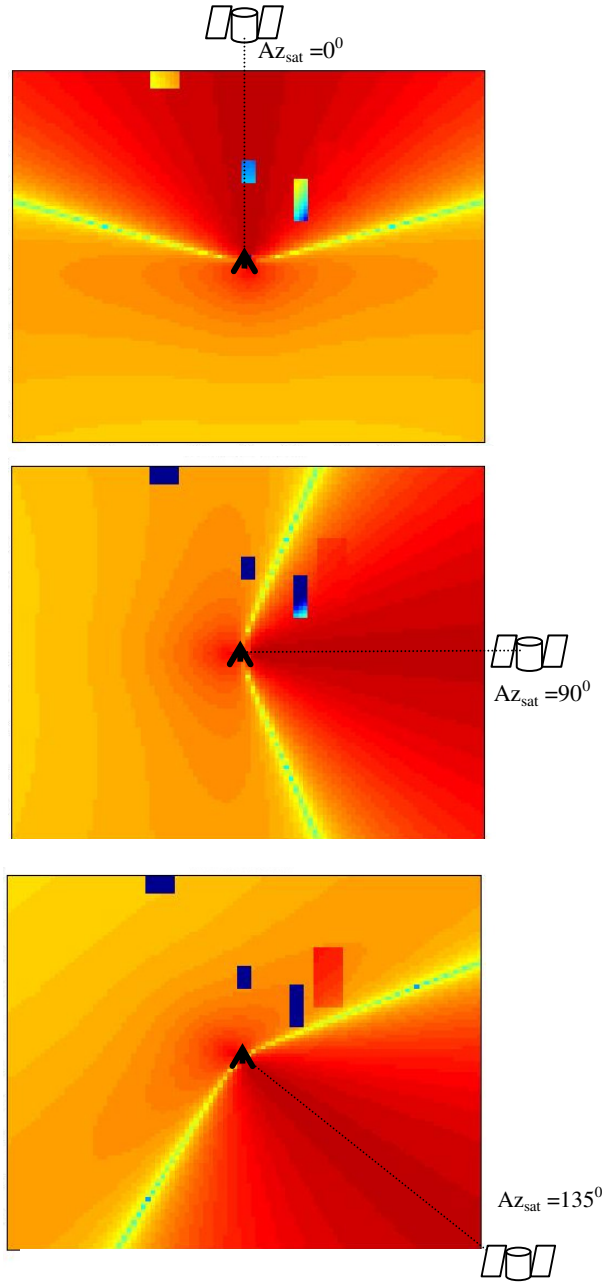

Figure 7. DBS bistatic scattering coefficients for test scene

These results demonstrate the potential utility of the simulation environment. In the simulation, the contrast between the scattered DBS signal from the rain event and the region surrounding the runway was quite low. This would imply that this sensor concept may have difficulty detecting haz-

ardous rain events for illumination angles from 135° to -135°. The next steps might be to add the reflected GPS signal and investigate the potential advantages of using dual Ku- and L-band bistatic measurements, as well as the impact of scattering geometry diversity provided by the GPS measurement. Such an investigation could be facilitated using the simulation environment described here.

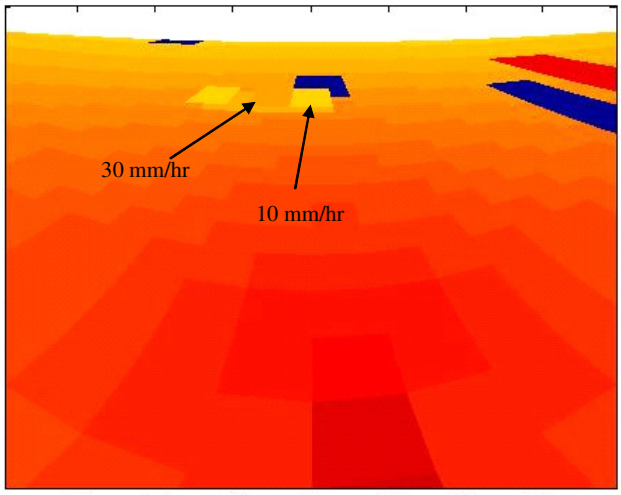

Figure 8. DBS scene with rain at runway threshold

Future Work

The initial effort discussed in this paper was focused on creating and demonstrating a simulation framework to investigate new aviation hazard-sensor concepts. However, in the future, additional modules will be designed to expand the capability of the tool for a wide variety of applications. A graphical interface is under development to simplify the editing of the EM characteristics of the surface. In addition, a scattering module more appropriate for smoother surfaces is also under development. Finally, while these results utilized MATLAB as the simulation engine, the modules will be converted to Octave and made available to other interested researchers for further development.

Summary

The objective of this effort was to develop and demonstrate a simulation environment to investigate advanced sensor concepts for aviation hazard detection. A model for atmospheric absorption due to water vapor and oxygen molecules, as well as a model to estimate the bistatic scattering coefficient from rough surfaces, were developed and compared to existing models. A rain-scattering model was adapted for use in this simulation. Although at present it includes only scattering and not attenuation due to rain, this model is useful for many geometries of interest. A MATLAB module to provide geometry utilities and provide the simulation geometry, such as aircraft location and surface structure, was also completed. These modules have been integrated and used for end-to-end simulation of the scattering environment.

These initial efforts are intended to lead to the development of a flexible MATLAB/OCTAVE-based microwave-simulation environment to enable the assessment of new microwave sensor concepts for the detection of aviation hazards. Present efforts to enhance the simulation environment with a rain-scattering model and smooth-surface scattering model are expected to enable the assessment of several bistatic radar-sensor concepts. The developed modeling environment provides the definition and initial development of an atmospheric propagation/microwave sensor-simulation tool that can be adapted, extended, and utilized by researchers for sensor/hazard investigations, and an assessment of a new radar-sensor technology for the detection of wind shear, runway incursion, and other aircraft in the terminal area.

References

[1] Howland,P.E, Maksimiuk, D.,& Reitsma, G.'FM radio based bistatic radar', IEE Proc,-Radar Sonar Navig., Vol. 152, No. 3, June 2005

[2] Chang, C. W., 'Television based bistatic radar, Technical report, University of Capetown, 2004

[3] Cherniakov, M., Kubik, K., and Nezlin, D., 'Radar sensors based on communications low Earth orbiting satellites,' IGARSS 2000, Honolulu Hawaii.

[4] Katzberg, S. J., and J. Dunion (2009), "Comparison of reflected GPS wind speed retrievals with dropsondes in tropical cyclones", Geophys. Res. Lett., 36, L17602.

[5] Nakagawa, K., Hanado, H. S. , Satoh, Takahashi, N. , Iguchi, T. , and Fukutani, K. ; 'Development of a new C-band bistatic polarimetric radar and observation of typhoon events,' 31st AMS Conference on Radar Meteorology, Vol. II, 863-866. 2003

[6] Ulaby, F.T., Moore, R.K., and Fung, A.K., Microwave remote sensing: Active and passive volume I Microwave Remote Sensing Fundamentals and Radiometry, Addison-Wesley Publishing, 1981

[7] Liebe, H.J and Dillion, T.A., Accurate Foreign Gas Broadening Parameters of the 22 GHz H2O Line from Refraction Spectroscopy, J. Chem. Phy., 50, pp. 727-732

[8] Meeks, M.L., and Lilley, A. E., The Microwave Spectrum of Oxygen in the Earth's Atmosphere, J. Geophys. Res., 68,pp.1683-1703, 1963

[9] Beckmann, P. and Spizzichino, A., The Scattering of Electromagnetic Waves from Rough Surfaces, Pergamon Press. Oxford, 1963
[10] Ulaby, F.T., Moore, R.K., and Fung, A.K., Microwave remote sensing: Active and passive volume III from theory to applications. Norwood: Artech House, 1986
[11] Mueller, E.A., and Jones, D.M., "Drop-size distributions in Florida". Proc. Eight Weather Radar Conf.,1960, Amer. Meteor. Soc.
[12] Wexler, R. and Atlas, D., "Radar Reflectivity and Attenuation of Rain", J. of Applied Meteor., Vol 2, April 1963.

Biography

ROLAND LAWRENCE is an assistant professor in the College of Engineering and Technology, the department of Engineering Technology at Old Dominion University. He instructs undergraduate courses electrical engineering technology, directs graduate research, and performs research involving advanced sensor concepts to enhance the safety of aircraft and the measurement capability to enable improved understanding of the Earth's environment. Dr. Lawrence can be reached at rlawrenc@odu.edu.